

Depth Distribution of Induced Radioactivity in Concrete Shield of Cyclotron Room

著者	Kimura K., Ishikawa T., Yamadera A., Nakamura T.
journal or publication title	CYRIC annual report
volume	1990
page range	255-258
year	1990
URL	http://hdl.handle.net/10097/49618

V. 3. Depth Distribution of Induced Radioactivity in Concrete Shield of Cyclotron Room

Kimura K., Ishikawa T.*, Yamadera A. and Nakamura T.*

*Cyclotron and Radioisotope Center, Tohoku University, *Technical Research Institute, Fujita Corporation*

Introduction

In accelerator facilities, the concrete, which is a structural and a radiation shielding material, is activated by neutrons produced from an accelerator. The radioactivity induced in the concrete causes radiation exposure to workers and increase of radioactive waste in decommissioning.

Many studies on induced activity in concrete have been reported for the irradiation experiments by thermal neutrons¹⁾, 14 MeV energy neutrons²⁾, and charged particles³⁾. There are, however, few data on induced activity measured in operating radiation facilities, and quite few data in the accelerator facilities.

We, therefore, measured induced activity of concrete in a cyclotron facility operated more than ten years.

Experiment

We bored samples from concrete side walls in the AVF cyclotron room at the Cyclotron and Radioisotope Center, Tohoku University(CYRIC). Four boring cores (5 cm diam. by 50 cm length) which were extracted at the same 1.25 m height from the floor as the cyclotron beam line, were cut into 2 cm thick disc-shaped samples. Figure 1 shows the schematic view of a cyclotron room and the position of the core boring (A to D). The gamma rays of radioisotopes induced in samples were measured with a pure Ge detector.

Result and Discussion

We identified eight radioactive nuclides of ^{46}Sc , ^{59}Fe , ^{60}Co , ^{65}Zn , ^{134}Cs , ^{152}Eu , ^{54}Mn and ^{22}Na in the concrete samples. The half lives and the dominant production reactions for these nuclides are shown in Table 1.

These nuclides can be divided into two groups. The isotopes of ^{46}Sc , ^{59}Fe , ^{60}Co , ^{65}Zn , ^{134}Cs and ^{152}Eu are produced by the (n, γ) reaction and ^{54}Mn and ^{22}Na are produced by high energy neutron reaction, i.e., (n, p) or $(n, 2n)$.

Figure 2 shows the distribution of saturated activities to the depth in the concrete wall at the point D. These values were obtained by correcting the measured data for irradiation time, cooling time, and self-absorption of samples. Figure 2 indicates the following facts,

- 1) The radionuclides induced by thermal neutrons through the (n, γ) reaction are dominant,
- 2) the induced activity by thermal neutron is highest at 5 to 10 cm depth rather than at the surface of concrete, and decreases rapidly according to the exponential function beyond about 20 cm depth,
- 3) the activity by high energy neutrons contributes a little to total activity, and it has a tendency to decrease monotonically from the concrete surface with the depth.

The distributions of ^{46}Sc saturated activities are shown in Fig. 3, and those of ^{54}Mn are shown in Fig. 4. In Fig. 3, the activities within 20 cm from concrete surface are nearly equal one another among the samples at the positions of A, C and D, and the activity of samples B is lower than those. In Fig. 4, the activity increases in the order of the samples B, A, C and D. This result means that thermal neutron fluence is nearly equal at the points A, C and D, but fast neutron fluence increases in the order of the positions B, A, C and D, since the ^{46}Sc is produced by thermal neutrons and Mn is produced by fast neutrons.

The activity distribution due to fast neutrons on the concrete surface indicated in Fig. 4 shows the similar tendency with that due to thermal neutrons within the concrete beyond about 20 cm depth as seen in Fig. 3, i.e., the activity has higher values in the order of the samples A, C, and D.

From these results, we can deduce the followings. At the point A, low energy neutrons produced by collision of the low energy accelerated particles leaked from accelerator has a main component, and a small fraction of these low energy neutrons arrive at the point B due to the shielding effect of the bulky cyclotron magnet. High energy neutrons are produced by collision of extracted particle after complete acceleration with the deflector or beam stopper and are dominant at the points C and D.

References

- 1) Evans J. C. et al., NUREG/cR-3474 (1984).
- 2) Oishi K. et al., Nucl. Sci. Eng. **103** (1989) 45.
- 3) Kondo K. et al., Health Phys. **46** (1984) 1221.

Table 1. Identified Nuclides in the Bored Concrete Samples

nuclide	reaction	half life
^{46}Sc	$^{45}\text{Sc}(n, \gamma) ^{46}\text{Sc}$	83.8 day
^{59}Fe	$^{58}\text{Fe}(n, \gamma) ^{59}\text{Fe}$	44.6 day
^{60}Co	$^{59}\text{Co}(n, \gamma) ^{60}\text{Co}$	5.271 year
^{65}Zn	$^{64}\text{Zn}(n, \gamma) ^{65}\text{Zn}$	244.1 day
^{134}Cs	$^{133}\text{Cs}(n, \gamma) ^{134}\text{Cs}$	2.062 year
^{152}Eu	$^{151}\text{Eu}(n, \gamma) ^{152}\text{Eu}$	13.3 year
^{54}Mn	$^{54}\text{Fe}(n, p) ^{54}\text{Mn}$	312.5 day
	$^{55}\text{Mn}(n, 2n) ^{54}\text{Mn}$	
^{22}Na	$^{23}\text{Na}(n, 2n) ^{22}\text{Na}$	2.602 year

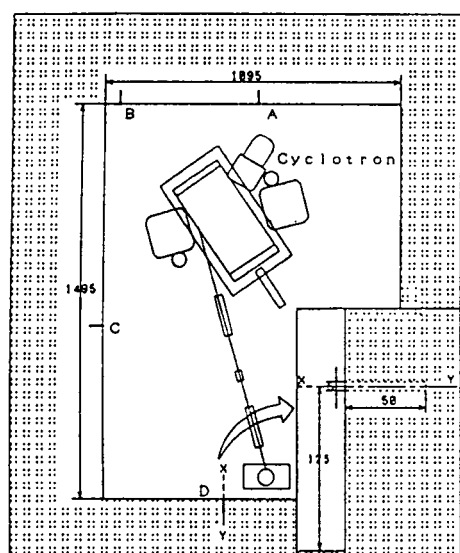


Fig. 1. Schematic View of a Cyclotron Room.

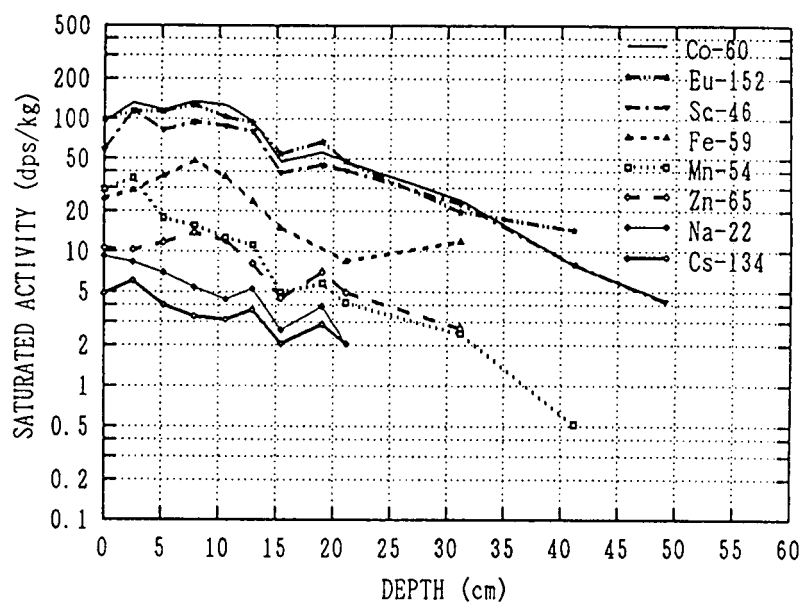


Fig. 2. Saturated Activity of the CYRIC Concrete Wall at the Position D

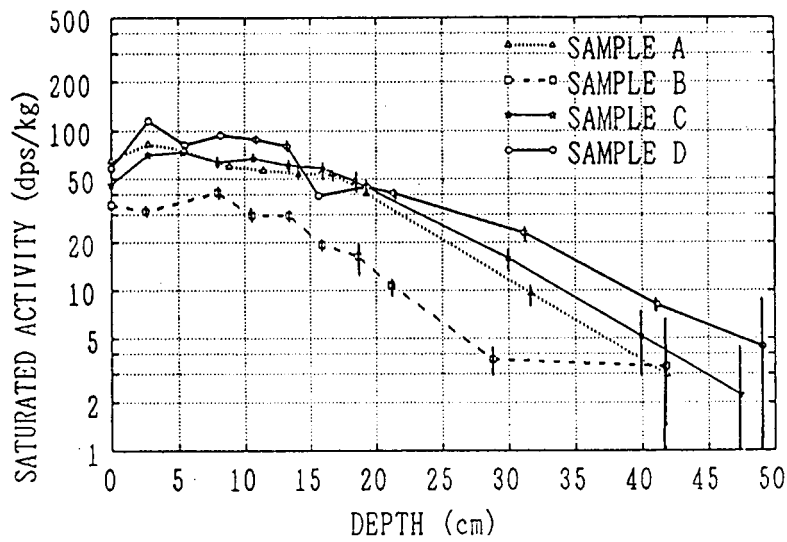


Fig. 3. Sc-46 Saturated Activity of the CYRIC Concrete Wall

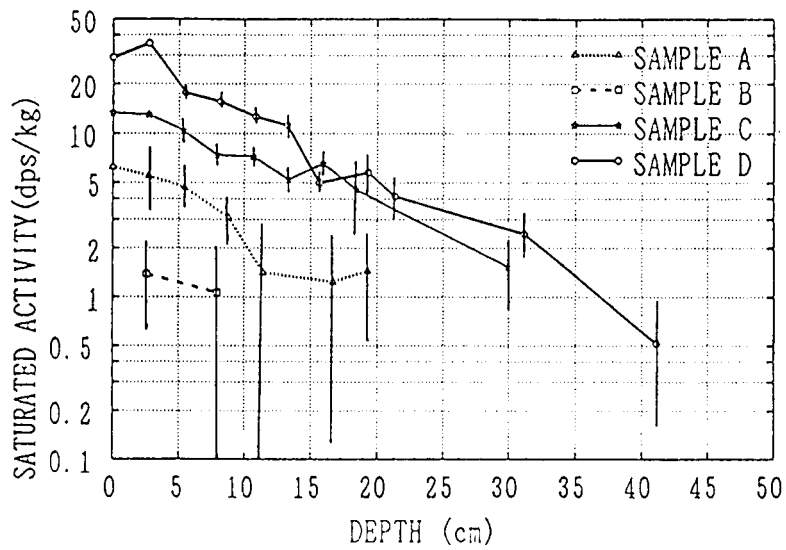


Fig. 4. Mn-54 Saturated Activity of the CYRIC Concrete Wall